Microchim Acta (2017) 184:3017–3025
DOI 10.1007/s00604-017-2305-1

ORIGINAL PAPER

Colorimetric and fluorometric detection of protamine by using a dual-mode probe consisting of carbon quantum dots and gold nanoparticles

Hanbing Rao[1] · Hongwei Ge[1] · Xianxiang Wang[1] · Zhaoyi Zhang[1] · Xin Liu[1] · Yan Yang[1] · Yaqin Liu[1] · Wei Liu[1] · Ping Zou[1] · Yanying Wang[1]

Received: 8 February 2017 / Accepted: 26 April 2017 / Published online: 13 May 2017

Abstract The paper describes an optical probe for colorimetric and fluorometric determination of protamine. The probe consists of a mixture of carbon quantum dots (CQDs) and gold nanoparticles (AuNPs) where the CQDs (with excitation/emission peaks at 350/440 nm) serve as fluorescent reporter and the AuNPs serve as a colorimetric reporter and a quencher of the fluorescene of CQDs. The nanoparticles applied here are characterized by high-resolution transmission electron microscopy (HRTEM), X-ray photoelectron spectroscopy (XPS), time correlated single photon counting (TCSPC), UV-vis and fluorescence spectroscopy, dynamic lights scattering (DLS) and zeta potentials. The green fluorescence of the CQDs overlaps the red absorption of AuNPs (520 nm) and therefore is quenched after fluorescence resonance energy transfer (FRET) between CQDs and AuNPs. Protamine is rich in basic arginine residues which are positively charged at physiological pH values. Protamine therefore can induce the aggregation of AuNPs which is accompanied by a color change from red to blue. Hence, the fluorescence of CQDs no longer overlaps the absorption of (aggregated) AuNPs (650 nm) and is not quenched as a result. These findings form the basis for a fluorometric assay that has linear response in the 10–220 ng·mL^{-1} protamine concentration range, with a 1.2 ng·mL^{-1} lower detection limit. The respective values for the colorimetric assay are 20–160 ng·mL^{-1} and 2 ng·mL^{-1}. This dual-signal probe also possesses excellent selectivity for protamine and in our perception has a large potential for the determination of protamine in serum.

Keywords Protein analysis · Competitive adsorption · FRET · Surface plasmon resonance

Introduction

Protamine is a low molecular weight protein (ca. 4500 Da) and has 20 positive charges (pI = 13.8) under physiological conditions [1, 2]. Protamine can be isolated from the sperm of salmon and other species of fish, and has been extensively used in clinical procedures. It can complex electrostatically with the sulfonate groups of heparin due to its high content of basic arginine residues [3]. In addition, it plays a biological role in binding DNA and providing a highly compact configuration of chromatin in the nucleus of sperm cells [4, 5]. Protamine is also an effective pharmaceutical compound that is used in cardiac surgery, vascular surgery and interventional radiology procedures [6]. However, its common unfavorable effects include sudden falls in blood pressure, pulmonary hypertension and dyspnea [7]. Therefore, it is vital to develop a rapid and accurate analytical method for protamine determination in serum samples.

Various analytical methodologies have been developed to provide a sensitive assay for protamine, including high performance liquid chromatography [8], microtiter plate-format optodes [9], electrochemical sensors [10], and fluorescence assays [6]. Among them, fluorometric [6, 11] and colorimetric methods [1] have been established for the quantification of protamine based on aggregation of AuNPs. An ultrasensitive

The authors wish it to be known that, in their opinions, Hanbing Rao and Hongwei Ge should be regarded as joint First Authors.

Electronic supplementary material The online version of this article (doi:10.1007/s00604-017-2305-1) contains supplementary material, which is available to authorized users.

✉ Yanying Wang
wyy@sicau.edu.cn

[1] College of Science, Sichuan Agricultural University, Ya'an 625014, People's Republic of China

fluorescence probe for protamine is based on the ability of AuNPs to quench the fluorescence of silicon quantum dots as well as the high binding affinity of protamine with AuNPs [11]. Ensafi et al. [6] developed a simple fluorescence probe for protamine detection based on the aggregation of GSH@CdTe quantum dots. Jena et al. reported a simple colorimetric method for sensing of protamine and heparin based on the reversible aggregation and disaggregation of AuNPs [1]. However, previously methods for detecting protamine only possess the ability to output a single signal, which is not convincing enough because many factors can interfere with the signal readout. Considering this, a new probe with a dual signal output should be constructed to achieve better performance.

A dual-mode colorimetric and fluorometric probe has opened up a new perspective for the design of bioassays. Compared with the single-signal assay, multi-signal sensing assays can offer more than one type of output mode simultaneously, thus making the detection results more convincing [12]. The dual-mode sensing system consists of fluorescent material and colorimetric indicator that also serves as fluorescence quencher. Yan et al. presented a dual-readout probe for folic acid based on gold nanoclusters and AuNPs [13]. Liu et al. [14] reported a bidimensional optical probe for arginine detection that was established by inhibiting the growth of AuNPs/CQDs composite. Cheng et al. presented a simple analytical system for detection of cyanide based on the fluorescent and colorimetric properties of FITC modified AuNPs [15]. As a result, dual-mode sensing systems show better performance than single-mode systems.

AuNPs have been widely applied in bioanalysis due to their excellent properties, such as size-dependent distinct color change, high fluorescence quenching efficiency and facile chemical modification [11, 16]. The surface plasmon resonance (SPR) and color of AuNPs are related to the interparticle distance. When the interparticle distance is higher than the average particle diameter, AuNPs appear red in color. When the interparticle distance becomes smaller than the average particle diameter, the red color of AuNPs changes to blue, due to aggregation [1]. This fascinating optical property of AuNPs make it an ideal colorimetric indicator, which generally displays different colors in visible range. Thus, AuNPs have been emerging as powerful assays in a variety of detection formats.

CQDs possess biocompatibility and unique photophysical and chemical properties, and they have been proven to be powerful as biocompatible inorganic fluorescent probes in chemical sensing and bioimaging [17, 18]. Thus, CQDs provide an exciting opportunity for alternative semiconductor quantum dots that are usually composed of toxic heavy metals (Te, Cd, Cu etc.) [19]. In addition, CQDs have promising potential to be a reducing agent, acting as electron donors [14, 20, 21]. According to previous reports, fluorescent assays based on CQDs have been used to detect ions [22], small molecules [23] and proteins [12], via fluorescence resonance energy transfer (FRET) and inner filter effect (IFE). These superiorities have driven the development of CQDs-based fluorescent assay.

Herein, we have developed a dual-mode probe with both colorimetric and fluorometric readouts for sensitive detection of protamine. The fluorescence of CQDs is significantly quenched in the presence of AuNPs. Protamine can induce aggregation of AuNPs through electrostatic interactions, resulting in the fluorescence of the CQDs being recovered. As a result, the colorimetric and fluorometric signals are effectively used for the sensitive detection of protamine. The dual-mode probe not only enables the visualization of protamine simply with bare eyes, but also provides a rapid, simple, and reliable assay.

Materials and methods

Materials

Ethylene diamine, sodium citrate, $CuSO_4·5H_2O$, citric acid ($C_6H_8O_7$), $FeCl_3·6H_2O$, (2-hydroxyethyl)-1-piperazineethanesulfonic acid (HEPES), NaOH, $CdCl_2$, $ZnCl_2$, $NiCl_2$, NaCl, $NaNO_3$, $AlCl_3$, NaF, KNO_3, K_2SO_4, $CoCl_2$, L-Pro, L-Ser, L-Met, L-His, L-Cys, $MgCl_2$, glutathione and glucose were purchased from Chengdu Kelong Chemistry Reagent Factory (Chengdu, China, http://www.cdkelong.com/). $HAuCl_4·3H_2O$ and protamine was purchased from Macklin (Shanghai, China, http://www.macklin.cn/). Procine Protamine ELISA Kit was purchased from Shanghai Jiang Lai Biological technology Co., Ltd. (Shanghai, China, http://www.laibio.com/). All chemicals were used as purchased, without further purification. Water used throughout all experiments was purified with a Millipore system (18.25 MΩ·cm).

Instrumentation

Fluorescence spectra was recorded with a PerkinElmer LS55 fluorescence spectrophotometer (America). UV-Vis spectra was recorded using an AnalytikJena Specord200Plus spectrophotometer (Germany). Photographs were taken with a commercial digital camera (China). XPS spectra were obtained with a Thermo ESCALAB 250XI Multifunctional photoelectron spectrometer (America). HRTEM measurements were carried out on a JEOL-2100F with an accelerating voltage of 200 kV (Japan). The fluorescence lifetimes were measured with a time-resolved fluorescence spectrometer model FLS 980 (UK). DLS and Zeta potential experiments were performed on a Malvern Zetasizer instrument (Malvern, Zetasizer Nano, UK).

Synthesis of photoluminescent CQDs and AuNPs

CQDs were synthesized using a hydrothermal processes with minor modification [24]. Briefly, 0.50 g of citric acid were dissolved in 12.5 mL distilled water and then mixed with 0.50 mL of ethylene diamine to form a transparent solution. Then, the solution was transferred into a 50 mL Teflon lined stainless autoclave. The sealed autoclave was heated to 160 °C in an electric oven and kept for additional 6 h before cooling down to room temperature naturally. The pale yellow solution obtained was stored in the refrigerator until used.

The colloidal solution of AuNPs was synthesized by means of citrate reduction of $HAuCl_4 \cdot 3H_2O$ [11, 25]. All glassware for the synthesis were thoroughly cleaned in aqua regia, rinsed with ultrapure water, and then oven-dried prior to use. Briefly, chloroauric acid solution (1 mL, 1% $HAuCl_4 \cdot 3H_2O$) was dropped into 50 mL distilled water. The solution was heated to boiling with vigorous stirring. Then, sodium citrate solution (1.8 mL, 1%) was rapidly added to the boiled $HAuCl_4 \cdot 3H_2O$ solution under stirring, resulting in a color change from light yellow to wine red. The reaction was then allowed to continue for an additional 15 min. After that, the heating mantle was removed, and stirring was continued without heating. After the solution cooled down to room temperature, the prepared AuNPs solution was filtered through a 0.45 μm membrane filter. The colloidal AuNPs were stored at 4 °C in a refrigerator until used.

UV-Vis and fluorescence detection of protamine

The protamine standard substance was dissolved in water to form a 4 $\mu g \cdot mL^{-1}$ solution. The prepared CQDs solution was diluted 5000 times. In a typical procedure, the mixed solution of CQDs/AuNPs was prepared using 450 μL of AuNPs, 20 μL of CQDs solution and HEPES buffer (10 mM, pH 7.16). Then various amounts of protamine standard solution were added to CQDs/AuNPs mixture solution, and the final volume was 4 mL. The mixture solution was vibrated and incubated at room temperature for 40 min. A sudden color change from red to blue was noticed after the addition of protamine. Finally, the mixture in quartz cuvette was transferred into quartz cuvette for UV-Vis scanning and fluorescence measurements. The fluorescence detection were under the uniform conditions: excitation wavelength and emission range were 355 and 380–600 nm, the slit widths of the excitation and emission were 10 nm and 15 nm, respectively. UV-Vis scanning was performed from 300 to 800 nm.

Detection of protamine in real samples

The proposed method was used to determine the content of protamine in porcine serum. The fresh porcine serum samples were collected and then centrifuged at 4000 rpm (1484 g) for 5 min to obtain the sera, which were diluted 100-fold before analysis. Protamine was dissolved in fresh porcine serum samples to a final concentration of 4 $\mu g \cdot mL^{-1}$. Then each spiked sample (50 μL, 100 μL, 120 μL) was added into the mixture solution containing the CQDs (20 μL) and AuNPs (450 μL), and the final volume was 4 mL. The mixture was vibrated and incubated at room temperature for 40 min. Finally, the mixture was transferred for UV-Vis scanning and fluorescence measurements.

Results and discussion

Synthesis and characterization

To obtain CQDs with amino-passivated surfaces, CQDs were prepared by a simple and environmentally friendly hydrothermal method with citric acid as the carbon source, and ethylenediamine as an effective passivating agent. The formation mechanism of CQDs is through a intermolecular dehydrolysis reaction and hydrothermal conditions promoted the reaction [24]. Additionally, the type of amine can significantly affect the fluorescent properties, and ethylenediamine is the best passivating agent for preparing of high photoluminescent CQDs [24]. Based on the above method, we synthesized highly photoluminescent CQDs using citric acid and ethylenediamine via a hydrothermal process.

The structural properties of the CQDs were characterized by HRTEM. HRTEM (Fig. 1a) image shows that the CQDs are nearly spherical and well separated from each other with a size 3.2 ± 0.62 nm. The HRTEM image of CQDs (inset of Fig. 1a) reveals high crystallinity with a lattice spacing of 0.35 nm, which agrees with the (002) crystal phase of graphite [24]. As shown in Fig. S1, it shows the FTIR spectra the of CQDs. There is stretching vibrational peak of –OH and $–NH_2$ at 3200–3400 cm^{-1} region, which improve stability and dispersibility in water. A shoulder peak at 1560 cm^{-1} is stronger, that can be assigned to the $–NH_2$. The stretching vibrational peak of of -C = O at 1645 cm^{-1} is hardly observed for CQDs. This indicates that CQDs possess more amino-groups [26].

The optical properties of prepared CQDs were investigated by fluorescence spectra and UV-Vis absorption spectra. The CQDs emit bright blue emission under ultraviolet radiation (365 nm) while appearing yellow transparent under daylight (inset of Fig. S2a). As shown in Fig. S2a, CQDs display a strong absorption band centered at 340 nm, and their characteristic absorption peak is similar to the excitation spectrum. The characteristic absorption peak is assigned to the contribution of surface groups and the π-π* transition [27]. The CQDs exhibit typical excitation-independent photoluminescence properties with increasing excitation wavelength in the range of 340–380 nm (Fig. S2a). Li et al. reported that amino-groups can achieve the controlled surface passivation of CQDs and

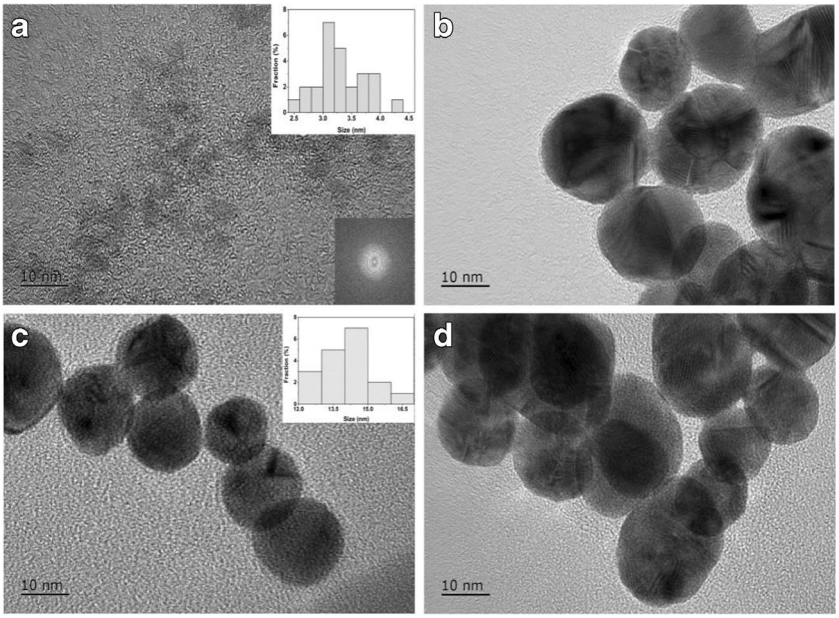

Fig. 1 **a** HRTEM images of CQDs, the inset was diffraction pattern of CQDs after FFT conversion. **b** HRTEM of AuNPs in presence of CQDs. **c** HRTEM images of free AuNPs. **d** HRTEM images of AuNPs in presence of protamine

determine the character of luminescence (excitation-dependent or independent) [26]. From Fig. S2a, excitation independent photoluminescent CQDs exhibit single exponential lifetime corresponding well with previous reports [24]. From Fig. S2b, the fluorescence intensity of CQDs remained high and almost constant in the pH range of 6–8.

Here, aqueous dispersions of AuNPs were synthesized by reduction of $HAuCl_4$ solution, using sodium citrate as both the reducing and protecting agent [11]. The AuNPs were characterized by HRTEM, XPS, DLS, Zeta potential and UV-Vis spectroscopy. HRTEM images are employed to characterize the morphology of AuNPs. As shown in Fig. 1c, AuNPs are globose in appearance with dispersed sizes, and the average particles size is 13.6 ± 0.57 nm (Fig. 1c). Further evidences are obtained by comparing the DLS data of corresponding solutions (Fig. S5a). The DLS data shows that the average hydrodynamic diameter of well dispersed AuNPs is 13.5 nm. The XPS survey spectrum (Fig. S2c) clearly showes two prominent peaks at approximately 84.5 eV and 88.0 eV, which are assigned to $Au4f_{7/2}$ and $Au4f_{5/2}$ for AuNPs, respectively. The binding energy of $Au4f_{7/2}$ between 84.0 eV and 87.8 eV revealed the coexistence of Au(0) and Au(I) in AuNPs. The zeta potential of AuNPs is determined to be −40.2 mV as depicted in Fig. S3, which reveal that the surface of synthesized AuNPs was negatively charged. This indicate that the AuNPs solution have good stability which is beneficial for storage, preservation and application.

The mechanism and detection strategy of probe

As shown in Fig. 2a, upon addition of AuNPs to a solution of CQDs, the fluorescence intensity of CQDs gradually decrease with increasing amounts of AuNPs. AuNPs were prepared by trisodium citrate as both the reducing and protecting agent, so the surface of AuNPs are rich in carboxyl group. Therefore, CQDs can bind with AuNPs through electrostatic interaction. As demonstrated in Fig. S6, the characteristic SPR peak of AuNPs at 520 nm decrease and a new peak at 650 nm increase with increasing concentrations (100 μL) of CQDs, indicate that CQDs directly induced the aggregation of AuNPs. From Fig. 1b, there is a compact "shell" on the surface of AuNPs, which indicated the presence of adsorbed CQDs. As shown in Fig. 2c, the absorbance band of the AuNPs overlapped with the emission spectrum of CQDs which indicate that the CQDs and the AuNPs constitute a donor-acceptor pair of a FRET system. Inner filter effect also requires spectral overlap, but the effect occurs if distances between emitted and re-absorber exceed 10 nm. In this system, there is no redox reaction. Based on the above mentioned, the main fluorescence quenching mechanism was FRET.

TCSPC was used to reveal the quenching mechanism of CQDs. From Fig. 2d, the fluorescence lifetime of CQDs is a single exponential decay. As shown in Table S1, the fluorescence lifetime of CQDs is 15.3 ± 0.5 ns when fit with a single exponential function. In addition, the lifetime of the aqueous solution of CQDs is 14.8 ± 0.4 ns with the AuNPs. This phenomenon supports a static quenching mechanism.

Figure 2e depicts the absorption spectra of CQDs, AuNPs, protamine, CQDs with AuNPs and CQDs/AuNPs with protamine. From Fig. 2e, it shows that there is no characteristic absorption of protamine, and AuNPs exhibite a SPR absorption band peak at 520 nm. Upon addition of protamine, the color of AuNPs suspension change from red to blue (Scheme 1**)**. The original absorbance of AuNPs at 520 nm decrease while a new absorbance peak at approximately 650 nm increase obviously, indicating that

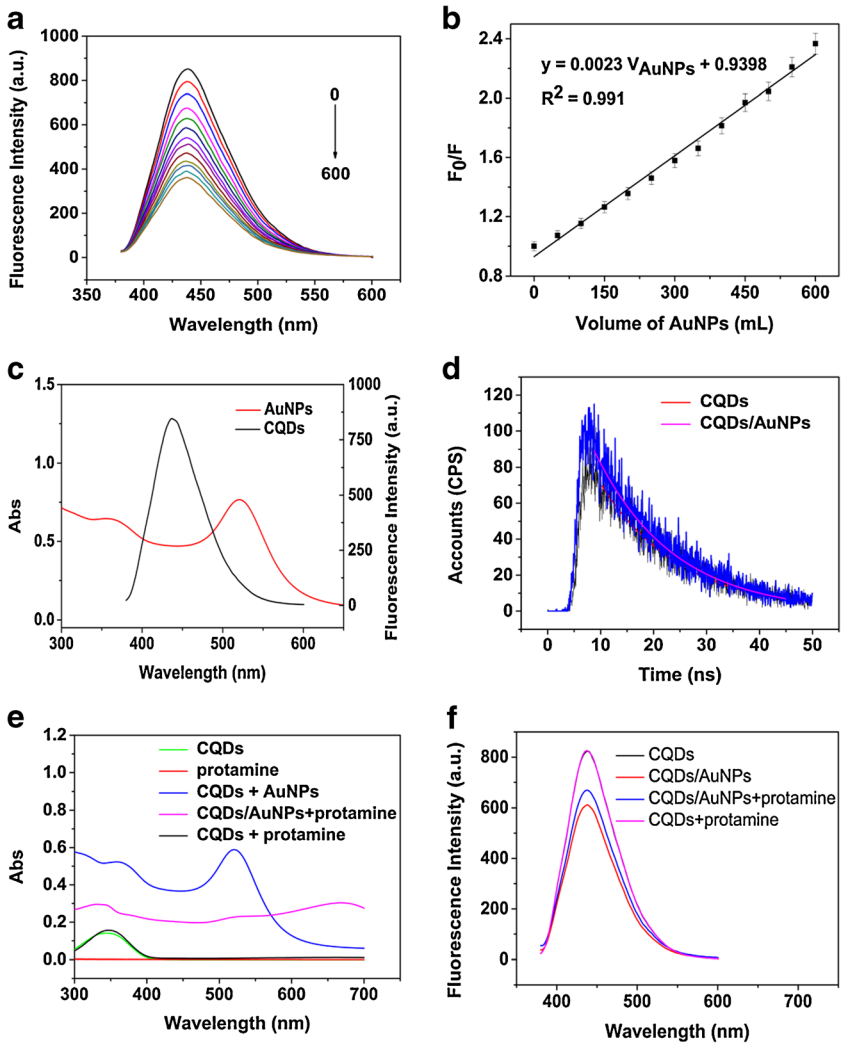

Fig. 2 **a** Fluorescence responses of the CQDs in the presence of different concentration of AuNPs. **b** The relationship between F/F_0 and the concentration of AuNPs ($n = 3$). The data is acquired at excitation/emission peaks of 350/440 nm. **c** UV–Vis absorption spectra of AuNPs and fluorescence spectroscopy of CQDs. **d** Fluorescence decays of CQDs and CQDs/AuNPs. **e** UV–Vis absorption spectra of CQDs, protamine, CQDs in the presence of protamine, AuNPs, CQDs/AuNPs in the presence of protamine. **f** Fluorescence spectroscopy of CQDs, CQDs/AuNPs, CQDs/AuNPs in the presence of protamine, CQDs in the presence of protamine

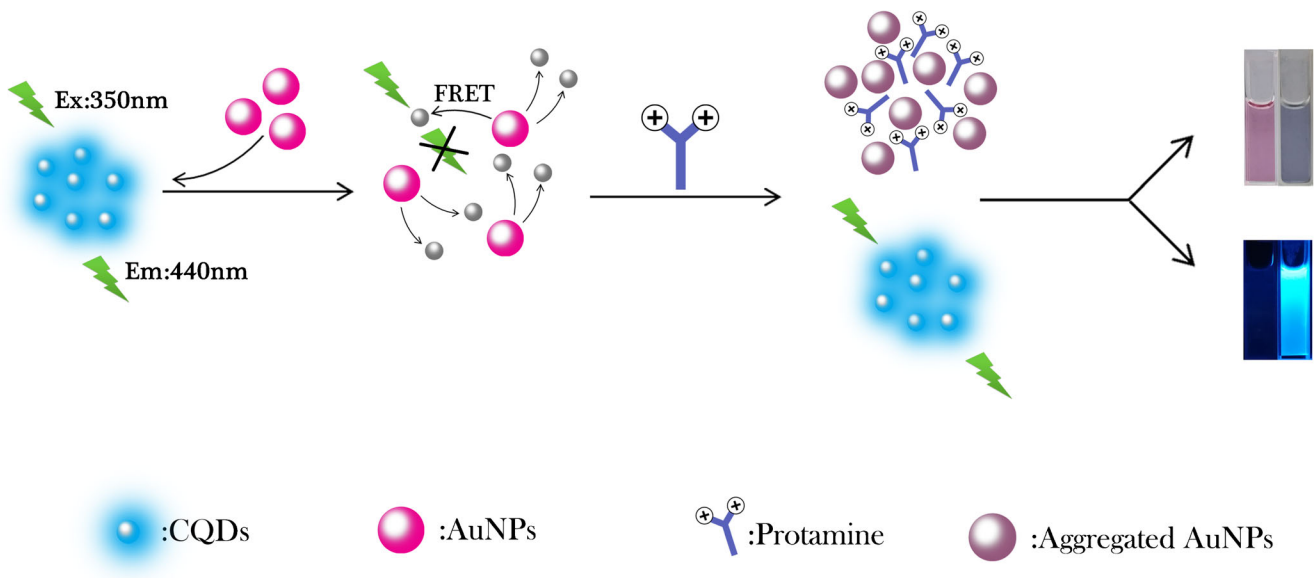

Scheme 1 The detection strategy of dual-mode probe for protamine

the aggregation of AuNPs are induced by protamine (Fig. 2e). Amine groups tend to readily adsorb onto the surface of AuNPs, and induce AuNPs to aggregate [1, 28]. As shown in Fig. 2e, the addition of protamine has negligible influence on the UV-Vis spectra of CQDs. As shown in Fig. 1d, it shows the aggregation of AuNPs by protamine. Further evidence was obtained by comparing the DLS and zeta potentials of corresponding solutions (Figs. S3, S4, S5). The DLS data shows that the average hydrodynamic diameter of well dispersed AuNPs is 13.5 nm, while that of the protamine induced aggregated AuNPs increased to 126.8 nm (Fig. S5). Moreover, the zeta potential of AuNPs increase significantly in the presence of protamine from −40.2 mV to −15.2 mV (Figs. S3, S4), which clearly shows that AuNPs aggregated through interaction with protamine.

Based on these findings, we proposed an original and dual-mode protocol by means of AuNPs and CQDs. As shown in Scheme 1, the AuNPs serve as a fluorescence quencher, which has been proved to possess an extraordinary quenching efficiency in a broad range of wavelengths [29]. Additionally, the AuNPs behave as a colorimetric indicator enabling colorimetric analysis. CQDs are readily adsorbed onto the surface of citrate stabilized AuNPs through electrostatic interaction, leading to fluorescence quenching of CQDs. However, protamine has stronger affinity toward AuNPs and can compete with CQDs to bind onto the surface of AuNPs with priority, which induce aggregation of AuNPs and fluorescence recovery of CQDs. Thus, the detection strategy is based on the competitive adsorption of protamine and CQDs on AuNPs. Both the colorimetric and fluorometric signals are useful for the detection of protamine. Based on this feature, excellent analytical performance for this dual-mode probe for protamine can be anticipated.

Optimization of method

In this study, the ratio of absorbance at 650 nm and 520 nm (A_{650}/A_{520}) is used to assess the degree of aggregation. A lower absorbance ratio indicates that AuNPs dispersed well in the solution, and a greater extent of AuNPs aggregates lead to a higher absorbance ratio. The fluorescence enhancement efficiency is defined as F_0/F, where F and F_0 correspond to the fluorescence intensity in the presence and absence of protamine, respectively.

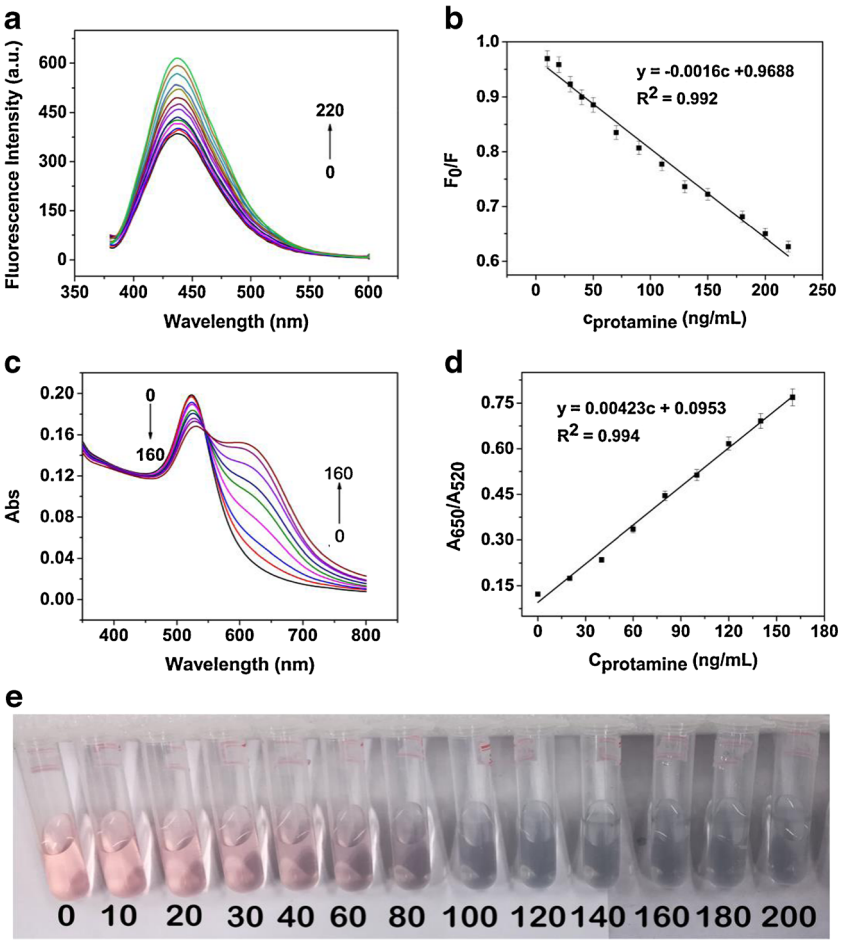

Fig. 3 **a** The fluorescence emission spectra of CQDs/AuNPs in the presence of different concentrations of protamine. **b** The relationship between F/F_0 and the concentration of protamine ($n = 3$). The data is acquired at excitation/emission peaks of 350/440 nm. **c** UV-Vis absorption spectra of the proposed assay in the presence of different amounts of protamine. **d** Relationship between the A_{650}/A_{520} ratio and the concentration of protamine ($n = 3$). The data is acquired at absorption peaks of 520 nm and 650 nm. **e** The photograph is the colorimetric response for various concentrations of protamine

Table 1 Comparison of various probes employed for protamine sensing

Probe	Methods	Linear detection range	Detection limit	Reference
Silicon quantum dots coupled with AuNPs	Fluorometric	0–1.2 μg·mL^{-1}	6.7 ng·mL^{-1}	[11]
AuNPs coupled with fluorophore	Fluorometric	0–0.8 μg·mL^{-1}	0.0067 μg·mL^{-1}	[30]
Folic acid capped AuNPs	Fluorometric	100 × 10^{-9}–1 × 10^{-12} g·mL^{-1}	4.8 × 10^{-15} g·mL^{-1}	[31]
FITC labeled DNA	Fluorometric	2.5–17.5 ng·mL^{-1}	2.2 ng·mL^{-1},	[5]
GSH-capped CdTe	Fluorometric	2.0–200 ng·mL^{-1}	1.0 ng·mL^{-1}	[6]
AuNPs	Colorimetric	0.1–1.5 μg·mL^{-1}		[1]
CQDs/AuNPs	Fluorometric and Colorimetric	10–220 ng·mL^{-1}	1.2 ng·mL^{-1}	This work

To optimize the method, the following parameters are optimized: (a) concentration of AuNPs; (b) pH of the medium; (c) reaction time. Respective data and figures are given in Fig.S7. We found the following experimental conditions to give best results:

(a) As shown in Fig. S7a, it is obvious that F/F_0 increases from 400 to 450 μL. When the volume of AuNPs exceeds 450 μL, the trend changes in the opposite direction. Significantly, excessive AuNPs can not be aggregated by protamine sufficiently and the dispersed AuNPs can quench the fluorescence of CQDs [12, 28]. From the Fig. S7b, the colorimetric responses reveal the similar results to fluorometric responses. According to the above analysis, 450 μL of AuNPs is chosen as the optimal volume for protamine detection.

(b) As shown in Fig. S7c, d, the effect of pH is examined using HEPES buffer in the range of 6.0–8.0. From Fig. S7c, F_0 increases with an increasing buffer pH values. This demonstrates that the quenching efficiency of AuNPs to CQDs reduces with the increasement of pH values. As shown in Fig. S7d, the values A_{650}/A_{520} of CQDs/AuNPs have negligible change, which indicates that CQDs/AuNPs are stable over the pH range of 6.8–8.0. It can be seen that the highest enhancement efficiency was obtained at a pH of 7.16 (Fig. S7c). Thus, a pH of 7.16 is chosen in this work.

(c) Figure S7e shows the time-dependent fluorescent response in the presence of protamine. The fluorescent enhancement efficiency maintain a stable value when the incubation time reaches 40 min. Thus, 40 min is chosen as the optimal incubation time in this work.

Sensitivity and selectivity for protamine detection

Under the optimum conditions discussed above, the probe's linear response range to protamine was measured. From Fig. 3a, it displays a gradual increase in fluorescence response at 440 nm with an increase in the concentration of protamine. It is clear that F_0/F exhibits a linear response to the protamine concentration in the range of 10–220 ng·mL^{-1} (Fig. 3b), and a detection limit based on 3δ/S was 1.2 ng·mL^{-1}. An increase in the concentration of protamine

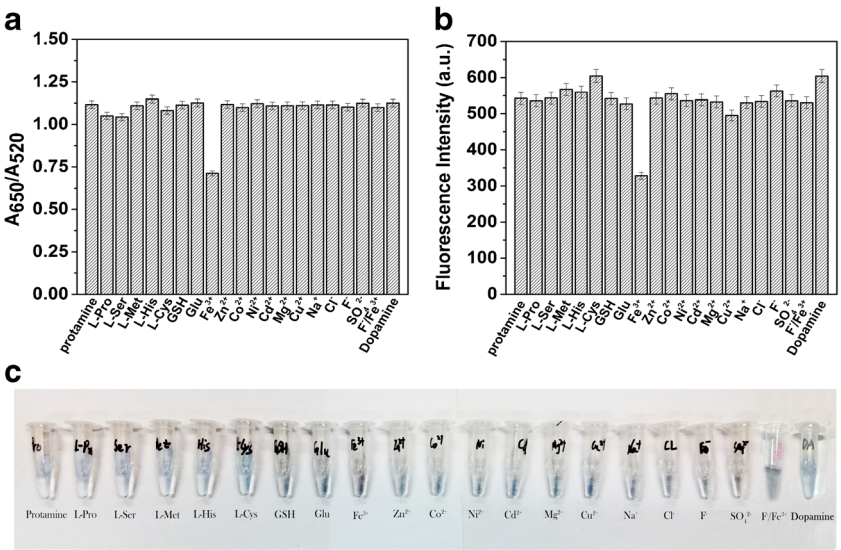

Fig. 4 **a** Absorbance response (A_{650}/A_{520}) of the CQDs/AuNPs probe in the presence of protamine or various metal ions at the concentration of 1 μM ($n = 3$). The data is acquired at absorption peaks of 520 nm and 650 nm. **b** The fluorescence intensity of CQDs/AuNPs in the presence of protamine or various ions and molecules at the concentration of 1 μM ($n = 3$). The data is acquired at excitation/emission peaks of 350/440 nm. **c** The photograph is the colorimetric response for various substances

results in the systematic increase of the absorbance at 650 nm and the decrease of the absorbance at 520 nm (Fig. 3c). As shown in Fig. 3d, it exhibits a good linear correlation ($R^2 = 0.994$) between relative absorbance A_{650}/A_{520} and the concentration of protamine in the range of 20–160 ng·mL^{-1}, and the detection limit of protamine based on 3δ/S is approximately 2 ng·mL^{-1}. Furthermore, both fluorescent and colorimetric methods show good linear relationships with protamine concentration. As shown in Fig. 3e, a distinguishable change in the color is observed by the bare eye. The color of solutions gradually changes from wine-red to blue with the increase of the concentration of protamine. The ptobe can exploit advantage of bare-eye detection and make the detection results more convincing. From Table 1, the reported methods for detecting protamine only output a single signal, which many factors can interfere with the signal readout. The present dual-mode probe for protamine makes the detection results more convincing and possesses a broad linear range and a low detection limit.

Then, the selectivity of this probe was investigated by screening the spectral responses toward various substances (Fig. 4**)**. The positively charges ions can interfere with protamine, as the proposed probe involved electrostatic interactions [1]. From Fig. (4a, b), the presence of Fe^{3+} can lead to significant spectral responses among the substances. We suspect that the carboxyl groups of AuNPs have a strong ability to Fe^{3+} in weakly basic medium. Fortunately, Fe^{3+} can be effectively eliminated by F^-. As shown in Fig. (4a, b), biomolecules have no interfere with the formation of CQDs/AuNPs composites under the same experimental conditions, and show little change in absorbance and fluorescence. In addition, remarkable selectivity can also be acquired by bare eye observation (Fig. 4c). The result further validates the idea that the proposed probe can serve as a "dual-mode" for detection of protamine.

Analysis of protamine in real sample

To evaluate the practicality of this method for the detection of protamine, the proposed probe was further evaluated with porcine serum samples. A series of known amounts of protamine were added into pretreated serum samples. The experiment is carried out with standard addition experiments. After that, the samples are tested by our developed method and a commercially available protamine ELISA kit. As shown in Table S2, the results indicate that recoveries of protamine reached to 84–110.00% and 86.50–105.00%, respectively. It is clear that our method is consistent with the commercial protamine ELISA kit. The results indicate that the proposed probe has great potential for applications in selectively determining protamine in serum samples.

Conclusions

In summary, this paper reports a probe for protamine that can be performed by fluorescent and colorimetric methods. A good linear relationship is obtained from 10 ng·mL^{-1} to 220 ng·mL^{-1} for protamine. The probe is successfully used to quantify protamine in porcine serum samples. This simple probe provides a reliable option for detecting protamine with sensitivity and selectivity. However, the probe is not suitable for samples containing polyionic molecular, oxidate substance and complex components. The proposed strategy may offer new potential applications in the fields of biosensing and biotechnology.

Acknowledgements This work was supported by a grant from the Two-Way Support Programs of Sichuan Agricultural University (Project No.03570113), the Education Department of Sichuan Provincial, PR China (Grant No. 16ZA0039). We thank the anonymous reviewers for their valuable suggestions.

Compliance with ethical standards The author(s) declare that they have no competing interests.

References

1. Jena BK, Raj CR (2008) Optical sensing of biomedically important polyionic drugs using nano-sized gold particles. Biosens Bioelectron 23(8):1285–1290
2. Shvarev A, Bakker E (2003) Reversible electrochemical detection of Nonelectroactive Polyions. J Am Chem Soc 125(37):11192–11193
3. Jaques LB (1979) Heparins–anionic polyelectrolyte drugs. Pharmacol Rev 31(2):99–166
4. Meistrich ML, Mohapatra B, Shirley CR, Zhao M (2003) Roles of transition nuclear proteins in spermiogenesis. Chromosoma 111(8):483–488
5. Pang S, Liu S, Su X (2014) A fluorescence assay for the trace detection of protamine and heparin. RSC Adv 4(49):25857–25862
6. Ensafi AA, Kazemifard N, Rezaei B (2015) A simple and rapid label-free fluorimetric biosensor for protamine detection based on glutathione-capped CdTe quantum dots aggregation. Biosens Bioelectron 71:243–248
7. Wakefield TW, Hantler CB, Lindblad B, Whitehouse WM Jr, Stanley JC (1986) Protamine pretreatment attenuation of hemodynamic and hematologic effects of heparin-protamine interaction: a prospective randomized study in human beings undergoing aortic reconstructive surgery. J Vasc Surg 3(6):885–889
8. Snycerski A, Dudkiewicz-Wilczynska J, Tautt J (1998) Determination of protamine sulphate in drug formulations using high performance liquid chromatography. J Pharmaceut Biomed 18(4–5):907–910
9. Kim SB, Kang TY, Cho HC, Choi MH, Cha GS, Nam H (2001) Determination of protamine using microtiter plate-format optodes. Anal Chim Acta 439(1):47–53
10. Xiao KP, Kim BY, Bruening ML (2001) Detection of protamine and heparin using electrodes modified with poly(acrylic acid) and its amine derivative. Electroanalysis 13(17):1447–1453
11. Peng X, Long Q, Li H, Zhang Y, Yao S (2015) "Turn on-off" fluorescent sensor for protamine and heparin based on label-free

silicon quantum dots coupled with gold nanoparticles. Sensors Actuators B Chem 213:131–138
12. Zhao D, Chen C, Sun J, Yang X (2016) Carbon dots-assisted colorimetric and fluorometric dual-mode protocol for acetylcholinesterase activity and inhibitors screening based on the inner filter effect of silver nanoparticles. Analyst 141(11):3280–3288
13. Yan X, Li H, Cao B, Ding Z, Su X (2015) A highly sensitive dual-readout assay based on gold nanoclusters for folic acid detection. Microchim Acta 182(7):1281–1288
14. Liu T, Li N, Dong JX, Zhang Y, Fan YZ, Lin SM, Luo HQ, Li NB (2017) A colorimetric and fluorometric dual-signal sensor for arginine detection by inhibiting the growth of gold nanoparticles/carbon quantum dots composite. Biosens Bioelectron 87:772–778
15. Cheng C, Chen H-Y, Wu C-S, Meena JS, Simon T, Ko F-H (2016) A highly sensitive and selective cyanide detection using a gold nanoparticle-based dual fluorescence–colorimetric sensor with a wide concentration range. Sensors Actuators B Chem 227:283–290
16. Zhang X, Yin J, Yoon J (2014) Recent advances in development of chiral fluorescent and colorimetric sensors. Chem Rev 114(9): 4918–4959
17. Liu Q, Xu S, Niu C, Li M, He D, Lu Z, Ma L, Na N, Huang F, Jiang H, Ouyang J (2015) Distinguish cancer cells based on targeting turn-on fluorescence imaging by folate functionalized green emitting carbon dots. Biosens Bioelectron 64:119–125
18. Gao X, Du C, Zhuang Z, Chen W (2016) Carbon quantum dot-based nanoprobes for metal ion detection. J Mater Chem C 4(29): 6927–6945
19. Ding C, Zhu A, Tian Y (2014) Functional surface engineering of C-dots for fluorescent Biosensing and in vivo Bioimaging. Accounts Chem Res 47(1):20–30
20. Strauss V, Margraf JT, Dolle C, Butz B, Nacken TJ, Walter J, Bauer W, Peukert W, Spiecker E, Clark T, Guldi DM (2014) Carbon Nanodots: toward a comprehensive understanding of their photoluminescence. J Am Chem Soc 136(49):17308–17316
21. Huang X, Zhang F, Zhu L, Choi KY, Guo N, Guo J, Tackett K, Anilkumar P, Liu G, Quan Q, Choi HS, Niu G, Sun Y-P, Lee S, Chen X (2013) Effect of injection routes on the Biodistribution, clearance, and tumor uptake of carbon dots. ACS Nano 7(7): 5684–5693
22. Zhang Y-L, Wang L, Zhang H-C, Liu Y, Wang H-Y, Kang Z-H, Lee S-T (2013) Graphitic carbon quantum dots as a fluorescent sensing platform for highly efficient detection of Fe3+ ions. RSC Adv 3(11):3733–3738
23. Dai H, Shi Y, Wang Y, Sun Y, Hu J, Ni P, Li Z (2014) A carbon dot based biosensor for melamine detection by fluorescence resonance energy transfer. Sensors Actuators B Chem 202:201–208
24. Qu D, Zheng M, Zhang L, Zhao H, Xie Z, Jing X, Haddad RE, Fan H, Sun Z (2014) Formation mechanism and optimization of highly luminescent N-doped graphene quantum dots. Scientific Reports 4:5294
25. Grabar KC, Freeman RG, Hommer MB, Natan MJ (1995) Preparation and characterization of Au colloid monolayers. Anal Chem 67(4):735–743
26. Li X, Zhang S, Kulinich SA, Liu Y, Zeng H (2014) Engineering surface states of carbon dots to achieve controllable luminescence for solid-luminescent composites and sensitive Be2+ detection. Scientific Reports 4:4976
27. Zhu S, Meng Q, Wang L, Zhang J, Song Y, Jin H, Zhang K, Sun H, Wang H, Yang B (2013) Highly Photoluminescent carbon dots for multicolor patterning, sensors, and Bioimaging. Angew Chem Int Ed 52(14):3953–3957
28. Lin F-e, Gui C, Wen W, Bao T, Zhang X, Wang S (2016) Dopamine assay based on an aggregation-induced reversed inner filter effect of gold nanoparticles on the fluorescence of graphene quantum dots. Talanta 158:292–298
29. Zhu J, Chang H, Li J-J, Li X, Zhao J-W (2017) Dual-mode melamine detection based on gold nanoparticles aggregation-induced fluorescence "turn-on" and "turn-off" of CdTe quantum dots. Sensors Actuators B Chem 239:906–915
30. Zhao J, Yi Y, Mi N, Yin B, Wei M, Chen Q, Li H, Zhang Y, Yao S (2013) Gold nanoparticle coupled with fluorophore for ultrasensitive detection of protamine and heparin. Talanta 116:951–957
31. Vasimalai N, John SA (2013) Aggregation and de-aggregation of gold nanoparticles induced by polyionic drugs: spectrofluorimetric determination of picogram amounts of protamine and heparin drugs in the presence of 1000-fold concentration of major interferences. J Mater Chem B 1(41):5620–5627